# Spin transition and symmetry-breaking in new mononuclear $Fe^{II}$ tren-complexes with up to 38 K hysteresis around room temperature†

Maksym Seredyuk,*[a,b] Kateryna Znovjyak,[a,b] Francisco Javier Valverde-Muñoz,[a] M. Carmen Muñoz,[c] Igor O. Fritsky,[b] Volodymyr M. Amirkhanov[b] and Jose A. Real *[a]

The structurally simple complex $\{Fe^{II}[tren(6F\text{-}py)_3]\}(BF_4)_2$ [tren(6F-py)$_3$ = tris(3-aza-4-(6-fluoro-2-pyridyl)-3-butenyl)amine] undergoes an abrupt spin transition (ST) with the critical temperature $T^{\downarrow}_{1/2}$ = 243 K on cooling and $T^{\uparrow}_{1/2}$ = 281 K on heating, with a 38 K wide hysteresis, while the $ClO_4^-$ congener shows ST spanning the room temperature region at $T^{\downarrow}_{1/2}$ = 267 K and $T^{\uparrow}_{1/2}$ = 295 K with a 28 K wide hysteresis. Calorimetric data confirm the occurrence of a highly energetic ST process, while multi-temperature single crystal X-ray structural studies identify a concerted symmetry-breaking $P2_1/n \leftrightarrow P2_1/c$ as the origin of the rare strong cooperativity and the large hysteresis loop. The analysis of the experimental data discloses two distinct interdependent events, namely, the combination of a gradual ST and an induced crystallographic phase transition, which endows the material with strong bistability and makes it an excellent platform for investigating new generations of ST based electronic and spintronic devices.

## Introduction

The study of responsive materials is an active research area having prospects for future and emerging technologies.[1] One of the well-known types of switchable molecular materials are pseudo-octahedral $Fe^{II}$ spin transition (ST) complexes, reversibly changing between the low-spin (LS) and high-spin (HS) electronic states by the action of physicochemical stimuli (temperature, pressure, light, chemical substrates, *etc.*) resulting in detectable and reversible variation of magnetic, spectral, electric, and dielectric properties, *etc.*[2] In view of the potential exploitation in technical devices as sensors,[1d,3] memory elements,[4] and micro- and nano-electro-mechanical[5] and energy harvesting systems[6] much effort has been made towards understanding the structure–function relationship for the purposeful tailoring of the ST characteristics and, particularly, achieving the most required hysteretic behaviour (or memory function).[2c,7] Application in real-life technical devices operating under ambient conditions, aside from the synthetic accessibility and chemical stability of materials, lays down constraints towards the hysteresis loop itself, which should be within the room temperature domain and resistant to cycling.[8] Also, from the viewpoint of possible technical exploitation, mononuclear ST complexes seem to be better suited since a number of techniques are available for relatively easy processability on micro-, nano- and single molecule-scales or in the form of films.[9]

In this regard, the desired hysteretic behaviour is a function of the adapted lattice packing and realized interactions between the ST molecules[10] that are reflected in polymeric[11] and supramolecular approaches to developing hysteretic ST materials.[12] Structure modifications due to polymorphism,[10] isomerisation[13] or phase transitions[14] are among the factors substantially affecting the ST parameters and cooperativity. In this respect, considerable internal lattice reorganization associated with the disorder of the lattice components simultaneously with ST has been recognized as an influential factor of hysteretic behaviour.[15]

Under certain circumstances, the changes accompanying the structure transformation lead to a change in the symmetry of the crystal lattice.[16] The symmetry-breaking event supporting ST is an unusual and unpredictable effect that requires a comprehensive approach to study, including high-quality structural data in both spin states. Only two fully structurally

[a]*Departament de Quimica Inorgànica, Institut de Ciencia Molecular (ICMol), Universitat de València, Valencia, Spain. E-mail: jose.a.real@uv.es*
[b]*Department of Chemistry, Taras Shevchenko National University of Kyiv, 64/13, Volodymyrska Street, 01601 Kyiv, Ukraine. E-mail: mcs@univ.kiev.ua, mlseredyuk@gmail.com*
[c]*Departamento de Fisica Aplicada, Universitat Politècnica de València, Camino de Vera s/n, 46022 Valencia, Spain*

† Electronic supplementary information (ESI) available. CCDC 2024798, 2024799 and 2091080. For ESI and crystallographic data in CIF or other electronic format see DOI: 10.1039/d1qi00941a

characterized complexes are currently known, namely $[Fe(PM\text{-}PEA)_2(NCSe)_2]$[17] and $[Fe(C_{10}\text{-}pbh)_2]$[18] (Fig. 1), for which symmetry-breaking underlies highly cooperative ST with a huge hysteresis loop. In the case of $[Fe(PM\text{-}PEA)_2(NCSe)_2]$, the ST with the hysteresis loop width $\Delta T_h$ = 41 K is concomitant with the change in the topology of intermolecular contacts and symmetry-breaking between orthorhombic *Pccn* (LS) and monoclinic $P2_1/c$ (HS) space groups. Similar crucial changes of the short contacts are observed for $[Fe^{II}(C_{10}\text{-}pbh)_2]$, which shows the ST transition of half of $Fe^{II}$ ions with $T^{\#="}_{1=2}$ = 268/303 K, $\Delta T_h$ = 35 K, along with the symmetry-breaking between monoclinic $P2_1/n$ (LS) and orthorhombic $P2_12_12$ (LS–HS) space groups.

As a result of our systematic work on tren-based $Fe^{II}$ ST complexes[9d,15j,k,19] we have serendipitously discovered new structurally simple and easily synthetically accessible complexes 1-$BF_4$ and 1-$ClO_4$ with the formula $\{Fe^{II}[tren(6F\text{-}py)_3]\}(BF_4/ClO_4)_2$ (tren(6F-py)$_3$ = tris(3-aza-4-(6-fluoro-2-pyridyl)-3-butenyl)amine) (Fig. 1) showing huge asymmetric ST hysteresis loops near room temperature. A detailed structural study revealed that symmetry-breaking with a change in the unit cell size accompanies the ST. The singular profile of this hysteresis behaviour was analysed using a model based on Landau theory of phase transitions. The modelling reveals two synchronized superimposed events, namely, a discontinuous crystallographic phase transition, which interrupts the inherent gradual ST and shapes an asymmetric ST hysteresis loop.

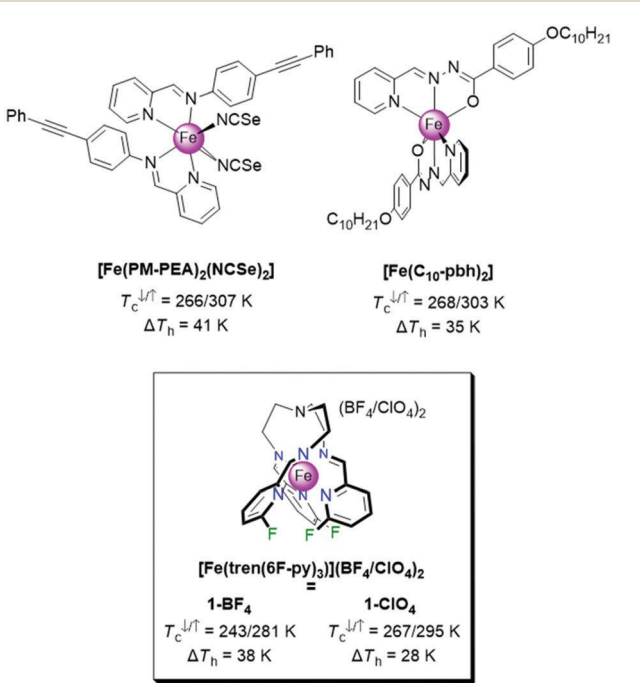


Fig. 1 Mononuclear complexes with a large ST hysteresis due to symmetry-breaking.

## Results

The title complexes were prepared by adding a solution of $Fe(BF_4)_2{\cdot}6H_2O$ or $Fe(ClO_4)_2{\cdot}nH_2O$ to the Schiff base obtained by condensation of 6-fluoropyridine aldehyde with tren (=tris(2-aminoethyl)amine) in absolute EtOH resulting in precipitation of black oily products. After standing for two weeks under the mother liquor, the oils completely transform into dark crystals of the respective complexes (see the ESI†).

The ST properties of the compounds were monitored through the thermal dependence of the $\chi_M T$ product recorded at 1 K $min^{-1}$ ($\chi_M$ is the molar magnetic susceptibility and $T$ is the temperature). In the low temperature region, the $\chi_M T$ value of 1-$BF_4$ corresponds to the LS state of the compound ($\chi_M T \approx 0$) (Fig. 2a). On heating, the susceptibility value gradually increases up to the value $\chi_M T$ = 0.68 $cm^3$ K $mol^{-1}$ at 273 K, corresponding to the fraction of HS complex molecules $\gamma_{HS} \approx 20\%$. On further heating an abrupt ST occurs, and the susceptibility increases up to a value 3.16 $cm^3$ K $mol^{-1}$ ($T^{"}_{1=2}$ = 281 K).

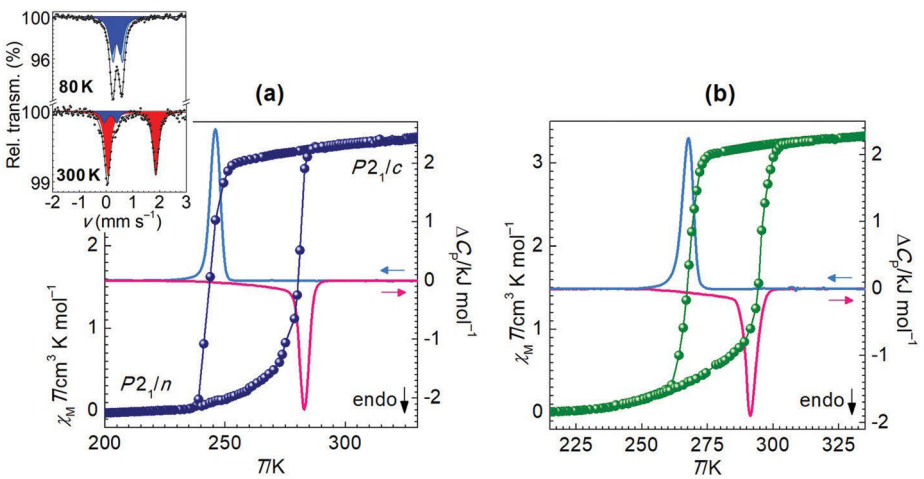


Fig. 2 Plot $\chi_M T$ *vs.* $T$ overlaid with $\Delta Cp$ curves for 1-$BF_4$ (a) and 1-$ClO_4$ (b). The inset shows the Mössbauer spectra of 1-$BF_4$ at the indicated temperature.

The susceptibility continues to slowly increase up to 3.40 $cm^3$ $K\,mol^{-1}$ on heating up to 400 K. Upon cooling, $x_MT$ shows a gradual decrease reaching a value *ca.* 3.00 $cm^3$ $K\,mol^{-1}$ at 250 K, and below this temperature abruptly drops to a value close to zero ($T^{\#}_{1=2}$ = 243 K). The shaped asymmetric hysteresis loop with a width $\Delta T_h$ = 38 K is moderately sensitive to the scan rate (Fig. S1†) and repeatable over successive thermal cycling without detriment but with a slight broadening (Fig. S2†).

For the isomorphous congener compound 1-$ClO_4$ (see a comparison of XRD profiles in Fig. S3†), the ST is characterized by $T^{\#}_{1=2}$ = 267 and $T^{"}_{1=2}$ = 295 K with the hysteresis $\Delta T_h$ = 28 K overlaying with the room temperature domain (283–303 K) (Fig. 2b). The change in the slope upon heating occurs at 290 K at $\gamma_{HS} \approx 0.3$. Opposite to 1-$BF_4$, the transition has a gradual character after the abrupt drop of the susceptibility on cooling. Overlaying the hysteresis loops of both compounds shows their close coincidence in the high- and low-temperature ranges, while the difference arises from the position of the hysteresis loops (Fig. S4†).

The observed upward shift of the ST curve when replacing $BF_4^-$ with $ClO_4^-$ suggests a stronger bonding/additional chemical pressure in 1-$ClO_4$ as a result of the increasing volume of the anion ($ClO_4^-$ is 24% larger by volume than $BF_4^-$ (ref. 20)). To support this hypothesis, we have investigated the effect of a small applied hydrostatic pressure on the ST behaviour of 1-$BF_4$. Already at a pressure of 0.42 kbar the hysteresis loop is shifted by 40 K up in temperature ($T^{\#="}_{1=2}$ = 280/322 K) and becomes more asymmetric with a larger contribution of the gradual part and the slope changes to almost vertical at $\gamma_{HS} \approx 30\%$ (Fig. 3). Also, the high temperature part of the curve becomes shifted down, reflecting the lowering of the spin conversion at high temperature due to the pressure effect.

The slightly asymmetric resonance signal in the Mössbauer spectrum of 1-$BF_4$ at 80 K was deconvolved with two LS doublets having different isomer shifts and quadrupole splitting values ($\delta^{LS1/LS2}$ = 0.38(2)/0.44(2) mm $s^{-1}$ and $\Delta E_Q^{LS1=LS2}$ = 0.32(2)/0.35(1) mm $s^{-1}$) with the relative areas $A$ in a ratio of 49(1) : 51(1) (Fig. 2a, inset). Evidently, the doublets correspond to two non-equivalent LS $Fe^{II}$ sites with slightly different geometric distortion of the coordination polyhedra. The best fit of the spectrum at 300 K gives a single HS doublet ($\delta^{HS}$ = 0.96(1) mm $s^{-1}$, $\Delta E_Q^{HS}$ = 1.80(2) mm $s^{-1}$) and a single LS doublet ($\delta^{LS}$ = 0.17(2) mm $s^{-1}$, $\Delta E_Q^{LS}$ = 0.47(2) mm $s^{-1}$) in a ratio of 86(3) : 14(3), which correlates with the incomplete ST transition at this temperature. On the other hand, the disappearance of the non-equivalency of $Fe^{II}$ sites in the same spin state and changing isomer shift and quadrupole splitting values of the partially preserved LS site suggest a phase transition in the course of the ST (see below).

The asymmetry of the hysteresis loops was addressed by a reversal curve (RC) study, a method allowing monitoring the development of cooperative interactions in the solid state.[21] We chose 1-$ClO_4$ as a model due to the higher asymmetry of the hysteresis loop compared to 1-$BF_4$. In the heating mode, independent of the reversal temperature and at any $\gamma_{HS}$ value, the RCs have a shape close to a rectangle that corresponds to the cooperative ST LS → HS (Fig. 4). However, upon cooling, the hysteretic behaviour is observed only above the reversal temperature 290 K, $\gamma_{HS} \approx 0.3$, while below it, the RCs are gradual and non-hysteretic. This threshold temperature corresponds to the point where the ascending curve becomes almost vertical (see Fig. 2 or 4). As mentioned above, for 1-$BF_4$ this point lays at a lower 273 K, $\gamma_{HS} \approx 0.2$.

Photogeneration of the metastable HS* state at low temperature, the so-called light induced excited spin state trapping (LIESST) experiment,[22] was carried out at 10 K by irradiating a microcrystalline sample of 1-$BF_4$ with red light (λ = 633 nm) for 5 h. Under these conditions the conversion to the HS* state is completed as follows from the attained $x_MT$ = 3.30 $cm^3$ $K\,mol^{-1}$ upon saturation, whereas on heating at 0.3 K $min^{-1}$ the compound relaxes back to the LS state with $T$ (LIESST) = 12.2 K (Fig. S5†). This very low $T$ (LIESST) value suggests a high $T_{1/2}$ value of the ST (see Discussion).

The heat capacity trace of 1-$BF_4$ at 5 K $min^{-1}$ has a peak at 279 K on heating and a peak at 244 K on cooling (Fig. 2a).[7] The average enthalpy and entropy values are 13.7 kJ $mol^{-1}$ and 53.0 J $K^{-1}$ $mol^{-1}$, respectively, and are characteristic of the cooperative $Fe^{II}$ systems. The entropy value is significantly higher than expected from electronic considerations (spin degeneracy only: $^1A_1 \rightarrow {}^5T_{2g}$ transition, $R\ln(5)$ = 13.4 J $K^{-1}$ $mol^{-1}$). The remaining entropy variation

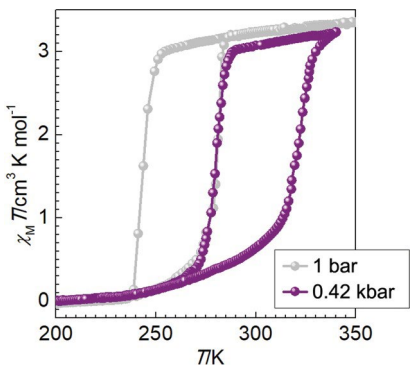


Fig. 3 Plot $x_MT$ *vs.* $T$ for 1-$BF_4$ under applied pressure.

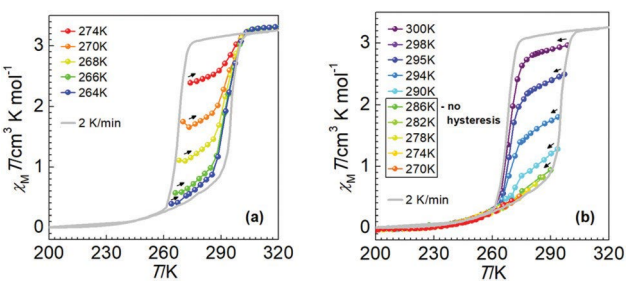


Fig. 4 Reversal curves for 1-$ClO_4$ upon heating (a) and cooling (b) at 2 K $min^{-1}$. The complete hysteresis loop at 2 K $min^{-1}$ is shown as a grey curve.

(53.0–13.4 = 39.6 J $K^{-1}$ $mol^{-1}$) accounts for the crystal and molecular vibrational modes involved in the ST process. For 1-$ClO_4$, the values are $\Delta H$ = 13.7 kJ $mol^{-1}$ and $\Delta S$ = 48.9 J $K^{-1}$ $mol^{-1}$ while the thermal anomalies are located at 292 K on heating and at 268 K on cooling (Fig. 2b). A closer look at the ascending $C_p$ curves of both compounds reveals two superimposed signals, corresponding to the gradual and steep parts of the ascending magnetic curves (Fig. S6†).

Single crystal X-ray analysis of 1-$BF_4$ at 280 K indicates that the unit cell has the monoclinic symmetry $P2_1/c$ and it changes to the $P2_1/n$ space group at 180 K with almost doubling the cell volume (Fig. S7 and Table S1†). The unit cell parameters $a$, $b$, and $c$ change on cooling: $\Delta a$ = +44.7% (or −9.6% for a half of the cell); $\Delta b$ = +3.8%; $\Delta c$ = +1.4% (Table S1†). The evolution of the crystal lattice parameters was also studied at different temperatures in the cooling and heating modes in the range 220–300 K with a 2 K interval. The thermal dependence of the unit cell volume $V$ matches the $\chi_M T$ *vs.* $T$ curve reasonably well, but the measured hysteresis is slightly narrower (32 K). This fact supports the idea that the ST behaviour of 1-$BF_4$ is a subject of sample texture and working on polycrystalline samples sometimes provides larger hysteresis.[17a,23]

To confirm the hysteresis width of the bulk polycrystalline material, powder X-ray diffractograms were collected in the range of the most intense diffraction peaks (2θ = 8–12.5°) at a variable temperature. The change in the intensity of the diffractograms upon heating and subsequent cooling (Fig. 5) clearly indicates the localization of the phase transition by temperature, which coincides with the dramatic change in magnetic susceptibility of the compound. The hysteresis loop width in the experimental quasi-stationary conditions is approximately 40 K, which also agrees well with the magnetic data.

The crystal structure of 1-$BF_4$ is comprised of $\{Fe^{II}[tren(6F\text{-}py)_3]\}^{2+}$ complex cations and two $BF_4^-$ anions balancing the charge (Fig. 6a). At 180 K, the unit cell contains two crystallographically distinct complex molecules [iron sites Fe(A) and Fe(B)] in the form of enantiomorphs of opposite chirality, and three ordered and one disordered $BF_4^-$ anions (Fig. S8a†). The $Fe^{II}$ ion is surrounded by three 6-fluoro-2-pyridinylimino moieties defining a pseudo-octahedral [$FeN_6$] coordination environment with an averaged distance <Fe–N> = 1.991(8) Å and the volume of the polyhedron $\langle V_{[FeN6]} \rangle$ = 10.303(8) $Å^3$. As shown by the minimized overlay (Fig. S8b†), the structural mismatch of the independent LS cations is in part due to the slightly different molecular shapes of the complex cations, whereas the major difference concerns the relative position of neighbouring anions, their orientation and the produced pattern of relevant intermolecular contacts below the van der Waals radii visualized in Fig. S8b† and by the colour-mapped Hirshfeld surface[24] in Fig. S9.†

The single crystal data at 265 K ($P2_1/n$), corresponding to a point on the gradual part of the ascending magnetic curve, show different transformation dynamics of the two complex molecules. As shown in Tables S2 and S3,† the Fe(B)-based molecule reveals a greater increase in Fe–N bond lengths than the Fe(A)-based molecule, while the average <Fe–N> value increases by 0.038 Å up to 2.029(8) Å, which is less than 18% increase in the $\gamma_{HS}$ value at this temperature that agrees well with the magnetic data. These data confirm that the gradual ST in the low-temperature region is also observed for single crystals of 1-$BF_4$, so the asymmetry of ST hysteresis is inherent to the compound and is not due to the texture effect.

At 280 K, due to the symmetry change, the independent cations and two pairs of anions become symmetry related, so that at this temperature the lattice is comprised of one unique complex cation and two distinct $BF_4^-$ anions (Fig. S10†). Due

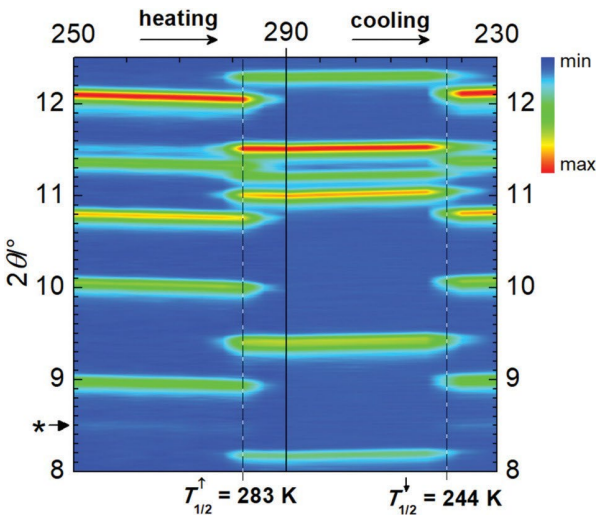


Fig. 5 Contour plot of X-ray powder diffractograms of 1-$BF_4$ in the range 2θ = 8–12.5° on heating and subsequent cooling. * – corresponds to the peak at 2θ ≈ 8.5° with (*hkl*) = (111).

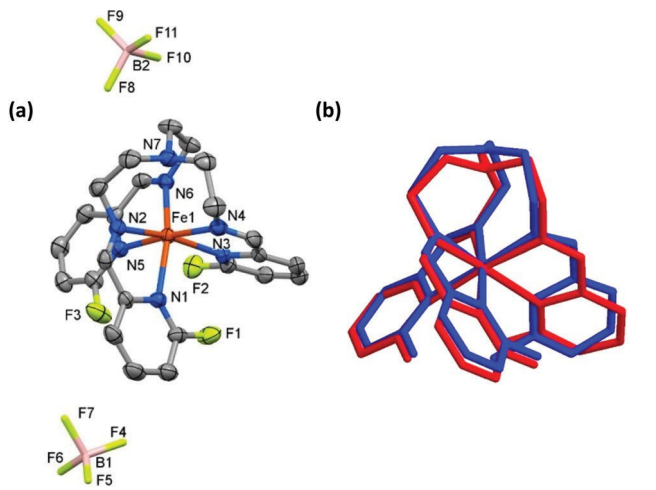


Fig. 6 (a) Projection of the complex cation and anions of 1-$BF_4$ at 280 K. Hydrogen atoms are omitted for clarity; (b) An overlay of the LS (blue, 180 K) and HS (red, 280 K) complex cations, demonstrating changed geometry due to the elongation of Fe–N bonds.

to the ST, the $V^{[FeN6]}$ increases up to 13.385(6) Å$^3$ (+30%), the distance <Fe–N> increases by 0.207 Å up to 2.198(6) Å. Due to the LS → HS transition, the coordination sphere expands (see Fig. 6b) and distorts as is clearly indicated by increasing distortion parameters (Table S3†). Comparison of the parameters of the LS 1-$BF_4$ with those of a similar methyl-substituted ST complex $\{Fe^{II}[tren(6Me\text{-}py)_3]\}(ClO_4)_2$,[19a] and the non-substituted non-ST LS complex $\{Fe^{II}[tren(py)_3]\}(ClO_4)_2$,[25] points out an intermediate position for the title compound in accordance with the reduced substituent size and decreasing steric crowding between pendant pyridine moieties in the series Me (2.00)[26] > F (1.47)[27] > H (1.20)[27] (in parentheses are the van der Waals radii in Å). Despite the tripod ligand, the trigonal prismatic distortion of the coordination environment is insignificant as follows from the large continuous shape measure values corresponding to the trigonal distortion CShM($D_{3h}$) and the small values corresponding to the octahedral geometry CShM($O_h$) (Table S3†). Therefore, for 1-$BF_4$ the polyhedron remains much closer to an octahedron in both spin states.

Although the crystal packing does not significantly change due to the ST as visualized by the minimized overlay of the LS and HS structures (Fig. S11†), several important changes take place. At 280 K, the lattice is formed by dimers of complex cations bound through the contact C2···C2′ below the van der Waals radii (= 3.178(8) Å) (Fig. S10†). The dimers are organized in bilayer assemblies extending in the *bc* plane and further interconnected through C···F–B contacts (= 3.078(8)–3.153(8) Å) with both $BF_4^-$ anions acting as bridges (Table S4†), and occupying the inner space of the bilayer (Fig. 7). No intermolecular contacts C···C or C···F exist between the successively stacked bilayers. In contrast, in the LS state at 180 K, due to the lattice contraction, the number of C···C contacts (= 3.126(9)–3.399(9) Å) increases, which results in the formation of a honeycomb-like supramolecular network of complex cations (Fig. S12†). The contacts C···F–B (= 3.051(9)–3.161(9) Å) bridge the successive networks into a 3D supramolecular structure. Alternatively, and for comparison purposes, in Fig. 7 the projections of the bilayer in *ab* and *bc* planes with both C···C and C···F–B contacts are shown. As is seen, the difference between the supramolecular organisations at both temperatures involves the relative spatial position of anions as well as the different complexity of the short intermolecular contacts in the lattice. Reconstruction of these networks during the ST event obstructs the transformation between the compact LS to the more voluminous HS complex cation, thereby resulting in a thermal lag of the ST transition for either heating or cooling processes. However, as follows from the magnetic data, the $T^{\uparrow}_{1/2}$ value of the ascending curve is more affected by the temperature scan rate (see Fig. S1b†). This observation suggests that the energy cost of the transformation from the compact LS

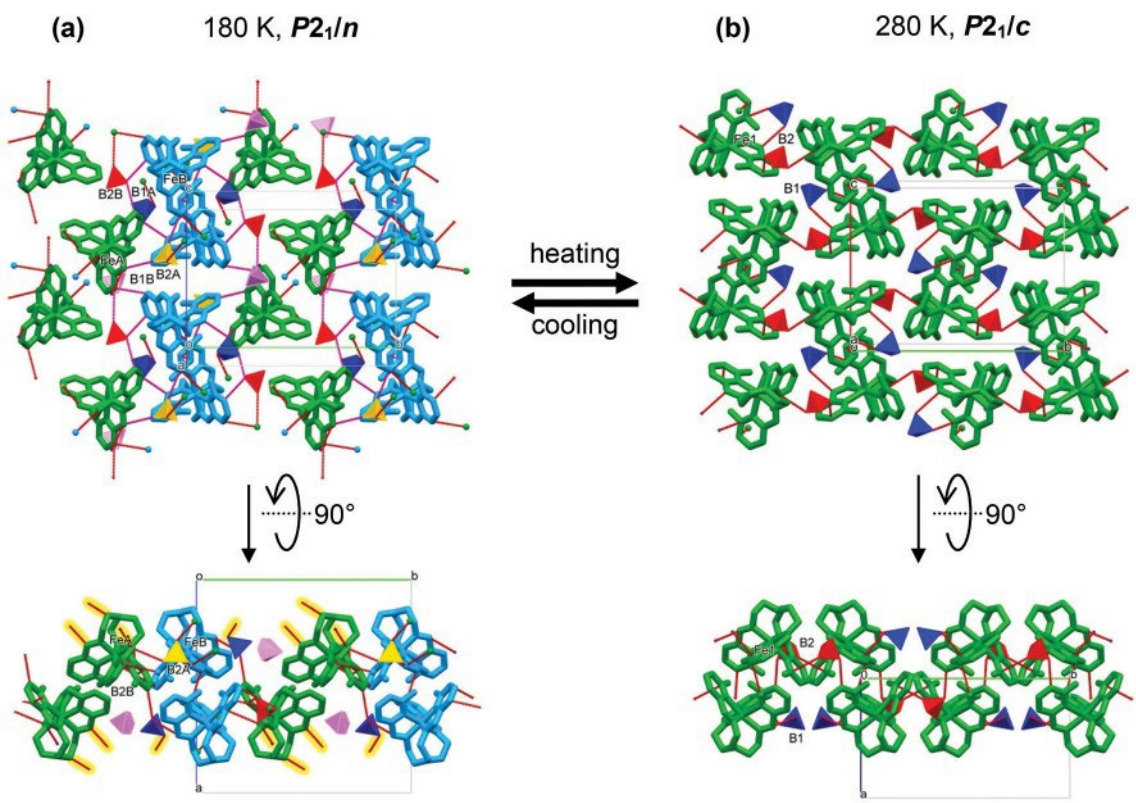


Fig. 7 Projection of the lattice packing in *bc* (a) and *ab* (b) planes at 180 and 280 K, correspondingly, for 1-$BF_4$ with intermolecular contacts drawn as red lines. The contacts between neighbouring bilayers are highlighted in yellow. Molecules and anions are colour mapped by symmetry equivalence.

phase with an extensive array of intermolecular contacts to the voluminous loosely connected HS phase is greater and hence a kinetically more hindered process than the reverse transformation as far as the $T^{\downarrow}_{1/2}$ value is less sensitive to the scan rate (Fig. S1b†).

## Discussion

In an almost semicentennial history of tren-based ST $Fe^{II}$ complexes, 1-$BF_4$ and 1-$ClO_4$ are the first to show a huge hysteresis around room temperature, which is, actually, also one of the largest reported for ST complexes with or without symmetry-breaking, structurally characterized in both spin states.[16b,17a,28] The origin of the hysteresis is purely structural and relates to a reorganization of the intermolecular interactions due to the phase transition. The important features of the title systems are the rigid nature of the compact ST molecule and anions and, on the other hand, the substantial similarities of the two lattice arrangements which, however, favor different spin states. Surprisingly enough, in neither arrangement strong stacking or H-bonds is observed, only the disorder of a single counterion.

An important point of this study is the asymmetry of the hysteresis loops of 1-$BF_4$ and 1-$ClO_4$, which suggests different mechanisms for the LS → HS and HS → LS transitions related to structural peculiarities of the HS and LS phases and their interconversion, while the hysteresis is due to the symmetry-breaking phase transition of the lattice at a critical concentration of the emerging new spin state species. A visual check of the asymmetric hysteretic curves of several symmetry-breaking ST systems (Fig. S13†) also hints at a gradual onset of ST up to a threshold concentration of HS/LS species, which farther develops as steep structural and spin state coupled transformations.

A number of phenomenological models were proposed for asymmetric ST hysteresis loops of different origins.[15b,29] Due to the coupling of ST and symmetry-breaking, we have chosen a model developed by Collet *et al.* and based on the Landau theory of phase transitions.[30] The basic idea of the model is to decompose the observed transition into the events of the intrinsic ST and the phase transition, which mutually influence each other through the volume strain. The potential energy of the system is expressed as a complex power series:

$$F(\eta; q; T) = \frac{1}{2}a\eta^2 + \frac{1}{4}b\eta^4 + \frac{1}{6}\eta^6 + Aq + \frac{1}{2}Bq^2 + \frac{1}{4}Cq^4 + Dq\eta^2;$$

where η is the symmetry-breaking order parameter; $q$ is the Ising spin transition order parameter (= $2\gamma_{HS} - 1$); $q\eta^2$ is the coupling term of both transitions; and $a$, $b$, $A$, $B$, $C$ and $D$ are numerical coefficients. The coefficients $a$ and $A$ are related to the critical temperature of the symmetry-breaking ($T_{SB}$) and intrinsic spin transition ($T_{IST}$), respectively, while the $b$ and $B$ define their character as discontinuous (if < 0) or gradual (if > 0).

The model can be used to reproduce the asymmetry of the experimental ST hysteresis loop using experimental structural data. We have chosen the Bragg peak (111) reflection of the low-temperature LS phase (Fig. 5), the intensity of which is proportional to the symmetry-breaking order parameter $\eta^2$ of the system.[30] One can note a synchronous change in the symmetry-breaking signal with a sharp change in $\gamma_{HS}$ (Fig. 8a), which confirms the synchronous occurrence of both events for the title compounds similarly, for example, to the complexes $[Co(dpzca)_2]$[31] and $[Fe(ptz)_6](BF_4)_2$,[32] the behaviour of which was successfully analysed in the frame of the model.[33]

The gradual onset of the spin transition on heating is considered to be due to the coupling term $Dq\eta^2$, which is non-zero when $\eta \neq 0$, *i.e.* in the low symmetry LS phase, and is zero in the high symmetry HS phase. Indeed, using the experimental intensity of the reflection (111) and considering the intrinsic gradual character of the ST (B > 0) we have successfully modelled the asymmetric hysteresis loop of 1-$BF_4$ (Fig. 8b). The $T_{IST}$ value of the high-temperature phase was set as 223 K which after renormalization due to coupling becomes $T_{IST\text{-}R}$ = 291 K for the low-temperature phase. For comparison, fitting the low- and high-temperature parts of the magnetic curve of both 1-$BF_4$ and 1-$ClO_4$ using the Slichter–Drickamer model[34] gives a comparable ST temperature $T_{SD\text{-}H}$ = 181 K for the high-temperature and $T_{SD\text{-}L}$ = 319 K for the low-temperature parts of the magnetic curve (Fig. S14†). Finally, the upward shift of $\eta^2$ in temperature increases the asymmetry of the curve that resembles the effect of external pressure on 1-$BF_4$ (Fig. 8c).

Several useful conclusions can be drawn:

• The photoexcitation of 1-$BF_4$ produces a HS* phase with a very low $T$ (LIESST) value. For tris(bidentate) $Fe^{II}$ complexes,[35] the $T$(LIESST) = 12.2 K should correspond roughly to $T_{1/2} \approx$ 360 K, *i.e.* well above the observed hysteresis. This can be explained by considering that the hysteresis is the result of the symmetry-breaking, whereas the low-temperature phase is characterized by non-cooperative ST behaviour with a high $T_{1/2}$

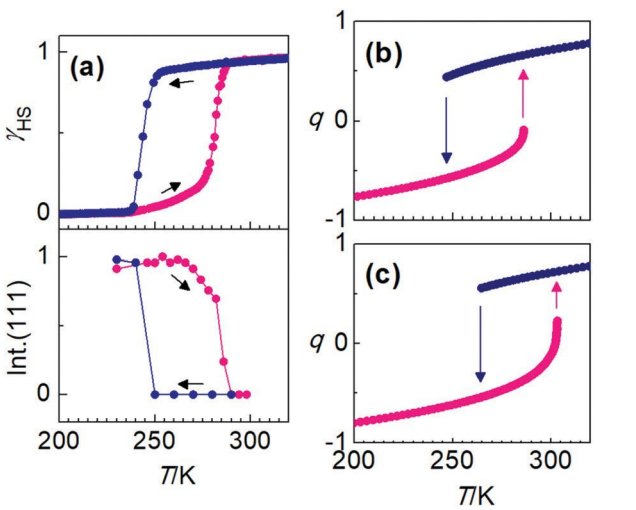


Fig. 8 (a) Synchronous change in the $\gamma_{HS}$ and symmetry-breaking signal; (b) Modelling the hysteresis of 1-$BF_4$ with experimental values of the (111) reflection; (c) increase of the gradual onset of ST due to the symmetry-breaking shifted upward in temperature.

value. The same can be concluded considering modelled values $T_{IST-R}$ or $T_{SD-L}$ above.

• Under external pressure, the observed counterintuitive incongruent thermal shift for the symmetry-breaking and gradual parts of the magnetic curves of 1-$BF_4$ and $[Co(dpzca)_2]$[36] or $[Fe(ptz)_6](BF_4)_2$[32] should be due to the higher volume variation for the concerted ST and symmetry-breaking in comparison with the gradual ST only.

• Substitution of $BF_4^-$ for the bulkier $ClO_4^-$ does not affect much the intrinsic gradual transition of the complex cations but exerts the effect similar to external pressure, *i.e.* shifts the symmetry-breaking upward in temperature and increases the gradual onset. Hence, the asymmetry of the hysteresis loop is governed by the relative position of the symmetry-breaking and of the intrinsic gradual ST. In the case of the title compounds, the higher the $T_{SB}$, the larger is the onset and the larger is the asymmetry.

The disentanglement of the structural and spin transitions is the first step towards controlling the macroscopic ST parameters of solid compounds which along with the robustness of thermal cycling and the easy processability of ST materials is a major challenge in front of the spin crossover community. Recently, we have demonstrated that it is possible to control the temperature, hysteresis width, and direction (forward or reverse) of ST in soft-matter $Fe^{II}$ complexes by means of the melting/crystallization process, whose temperature of occurrence is defined by the length of the aliphatic substituents.[9d,14,19b,37] Although the nature of 1-$BF_4$ and 1-$ClO_4$ is different, the tetrahedral anions play a role similar to that of the aliphatic chains, determining the temperature of the symmetry-breaking transition, which dramatically changes the evolution of the ST. In this particular case, the scarce number of singly charged tetrahedral anions limits further studies, but, fortunately, for 1-$ClO_4$ the hysteretic ST is superimposed on the technologically important room temperature region.

## Conclusions

In summary, we have discovered and scrutinized structurally simple $Fe^{II}$ complexes undergoing abrupt ST close to or within the room temperature domain with an impressive and perfectly repeatable hysteresis up to 38 K. Structural studies indicate that the hysteresis is driven by a symmetry-breaking phase transition halving/doubling the unit cell.

Given the tendency of substituted $Fe^{II}$ tren-based and other systems to show solid–solid phase transitions we expect to report more ST systems with excellent fine-tunability dependent on peripheral groups. Efforts along this line are already underway in our laboratories.

## Conflicts of interest

There are no conflicts to declare.

## Acknowledgements

This work was supported by grant PID2019-106147GB-I00 funded by MCIN/AEI/10.13039/501100011033, Unidad de Excelencia María de Maeztu (CEX2019-000919-M); the Generalitat Valenciana through PROMETEO/2016/147 and EU Framework FET-OPEN project COSMICS (grant agreement 766726), by the grant of the Ministry of Education and Science of Ukraine for perspective development of a scientific direction "Mathematical sciences and natural sciences" at Taras Shevchenko National University of Kyiv. We thank Prof. Dr Eric Collet for invaluable comments and suggestions.

## References

1 (*a*) S.-y. Koshihara, Photo-induced phase transition: from where it comes and to where it goes?, *J. Phys.: Conf. Ser.*, 2005, 21, 7; (*b*) K. H. Bennemann, Photoinduced phase transitions, *J. Phys.: Condens. Matter*, 2011, 23, 073202; (c) O. Sato, Dynamic molecular crystals with switchable physical properties, *Nat. Chem.*, 2016, 8, 644–656; (d) K. S. Kumar and M. Ruben, Emerging trends in spin crossover (SCO) based functional materials and devices, *Coord. Chem. Rev.*, 2017, 346, 176–205.

2 (*a*) P. Gütlich, A. Hauser and H. Spiering, Thermal and optical switching of iron(II) complexes, *Angew. Chem., Int. Ed.*, 1994, 33, 2024–2054; (*b*) *Spin crossover in transition metal compounds I-III*, ed. P. Gütlich and G. Goodwin, Top. Curr. Chem., vol. 233, 234, 235, 2004; (*c*) *Spin-Crossover Materials: Properties and Applications*, ed. M. A. Halcrow, John Wiley & Sons Ltd, Chichester, 2013.

3 A. Lapresta-Fernández, M. P. Cuéllar, J. M. Herrera, A. Salinas-Castillo, M. d. C. Pegalajar, S. Titos-Padilla, E. Colacio and L. F. Capitán-Vallvey, Particle tuning and modulation of the magnetic/colour synergy in Fe(II) spin crossover-polymer nanocomposites in a thermochromic sensor array, *J. Mater. Chem. C*, 2014, 2, 7292–7303.

4 A. Bousseksou, C. Vieu, J.-F. Létard, P. Demont, J.-P. Tuchagues, L. Malaquin, G. Menegotto and L. Salmon, *EU Patent*, 1430552, 2004.

5 (*a*) M. D. Manrique-Juarez, S. Rat, L. Salmon, G. Molnar, C. M. Quintero, L. Nicu, H. J. Shepherd and A. Bousseksou, Switchable molecule-based materials for micro- and nanoscale actuating applications: Achievements and prospects, *Coord. Chem. Rev.*, 2016, 308, 395–408; (*b*) M. Urdampilleta, C. Ayela, P. H. Ducrot, D. Rosario-Amorin, A. Mondal, M. Rouzieres, P. Dechambenoit, C. Mathoniere, F. Mathieu, I. Dufour and R. Clerac, Molecule-based microelectromechanical sensors, *Sci. Rep.*, 2018, 8, 8016.

6 M. Piedrahita-Bello, L. Salmon, G. Molnar, P. Demont, B. Martin and A. Bousseksou, Mechano-electric coupling in P(VDF-TrFE)/spin crossover composites, *J. Mater. Chem. C*, 2020, 8, 6042–6051.

7 S. Brooker, Spin crossover with thermal hysteresis: practicalities and lessons learnt, *Chem. Soc. Rev.*, 2015, 44, 2880–2892.

8 M. A. Halcrow, Structure:function relationships in molecular spin-crossover complexes, *Chem. Soc. Rev.*, 2011, 40, 4119–4142.

9 (*a*) N. Daro, L. Moulet, N. Penin, N. Paradis, J.-F. Letard, E. Lebraud, S. Buffiere, G. Chastanet and P. Guionneau, Spray-Drying to Get Spin-Crossover Materials, *Materials*, 2017, 10; (*b*) M. Ruben and K. S. Kumar, Sublimable Spin Crossover Complexes: From Spin-State Switching to Molecular Devices, *Angew. Chem., Int. Ed.*, 2021, 60, 7502–7521; (*c*) A. Tissot, J.-F. Bardeau, E. Riviere, F. Brisset and M.-L. Boillot, Thermo- and photoswitchable spin-crossover nanoparticles of an iron(II) complex trapped in transparent silica thin films, *Dalton Trans.*, 2010, 39, 7806–7812; (*d*) M. Seredyuk, M. C. Muñoz, V. Ksenofontov, P. Gütlich, Y. Galyametdinov and J. A. Real, Spin crossover star-shaped metallomesogens of iron(II), *Inorg. Chem.*, 2014, 53, 8442–8454.

10 J. Tao, R.-J. Wei, R.-B. Huang and L.-S. Zheng, Polymorphism in spin-crossover systems, *Chem. Soc. Rev.*, 2012, 41, 703.

11 (*a*) K. S. Murray and C. J. Kepert, Cooperativity in spin crossover systems: Memory, magnetism and microporosity, *Top. Curr. Chem.*, 2004, 233, 195–228; (*b*) O. Kahn and J. Martinez, Spin-transition polymers: From molecular materials toward memory devices, *Science*, 1998, 279, 44–48.

12 (*a*) P. Gütlich and H. A. Goodwin, Spin crossover - An overall perspective, *Top. Curr. Chem.*, 2004, 233, 1–47; (b) B. Weber, W. Bauer and J. Obel, An Iron(II) Spin-Crossover Complex with a 70 K Wide Thermal Hysteresis Loop, *Angew. Chem., Int. Ed.*, 2008, 47, 10098–10101; (c) A. Abhervé, M. Clemente-León, E. Coronado, C. J. Gómez-García and M. López-Jordà, A spin-crossover complex based on a 2,6-bis( pyrazol-1-yl)pyridine (1-bpp) ligand functionalized with a carboxylate group, *Dalton Trans.*, 2014, 43, 9406; (*d*) Z. J. Zhong, J. Q. Tao, Z. Yu, C. Y. Dun, Y. J. Liu and X. Z. You, A stacking spin-crossover iron(II) compound with a large hysteresis, *J. Chem. Soc., Dalton Trans.*, 1998, 3, 327–328.

13 (*a*) Y. Hasegawa, K. Takahashi, S. Kume and H. Nishihara, Complete solid state photoisomerization of bis(dipyrazolyl-styrylpyridine)iron(II) to change magnetic properties, *Chem. Commun.*, 2011, 47, 6846–6848; (*b*) Y. Hasegawa, R. Sakamoto, K. Takahashi and H. Nishihara, Bis[(E)-2,6-bis(1H-pyrazol-1-yl)-4-styrylpyridine]iron(II) Complex: Relationship between Thermal Spin Crossover and Crystal Solvent, *Inorg. Chem.*, 2013, 52, 1658–1665; (*c*) B. Rösner, M. Milek, A. Witt, B. Gobaut, P. Torelli, R. H. Fink and M. M. Khusniyarov, Reversible Photoswitching of a Spin-Crossover Molecular Complex in the Solid State at Room Temperature, *Angew. Chem., Int. Ed.*, 2015, 54, 12976–12980.

14 T. Romero-Morcillo, M. Seredyuk, M. C. Muñoz and J. A. Real, Meltable spin transition molecular materials with tunable $T_c$ and hysteresis loop width, *Angew. Chem., Int. Ed.*, 2015, 54, 14777–14781.

15 (*a*) D. Chernyshov, M. Hostettler, K. W. Törnroos and H. B. Bürgi, Ordering phenomena and phase transitions in a spin-crossover compound-uncovering the nature of the intermediate phase of $[Fe(2\text{-pic})_3]Cl_2{\cdot}EtOH$, *Angew. Chem., Int. Ed.*, 2003, 42, 3825–3830; (*b*) K. W. Törnroos, M. Hostettler, D. Chernyshov, B. Vangdal and H. B. Bürgi, Interplay of spin conversion and structural phase transformations: Re-entrant phase transitions in the 2-propanol solvate of tris(2picolylamine)iron(II) dichloride, *Chem. – Eur. J.*, 2006, 12, 6207–6215; (*c*) D. Chernyshov, B. Vangdal, K. W. Tornroos and H. B. Burgi, Chemical disorder and spin crossover in a mixed ethanol-2-propanol solvate of Fe-II tris(2-picolylamine) dichloride, *New J. Chem.*, 2009, 33, 1277–1282; (*d*) G. S. Matouzenko, D. Luneau, G. Molnar, N. Ould-Moussa, S. Zein, S. A. Borshch, A. Bousseksou and F. Averseng, A two-step spin transition and order-disorder phenomena in the mononuclear compound $[Fe(Hpy\text{-}DAPP)](BF_4)_2$, *Eur. J. Inorg. Chem.*, 2006, 2671–2682; (*e*) S. Lakhloufi, P. Guionneau, M. Lemée-Cailleau, P. Rosa and J. F. Létard, Structural phase transition in the spin-crossover complex $[Fe(ptz)_6](BF_4)_2$ studied by X-ray diffraction, *Phys. Rev. B: Condens. Matter Mater. Phys.*, 2010, 82, 132104; (*f*) H. Hagiwara and S. Okada, A polymorphism-dependent T-1/2 shift of 100 K in a hysteretic spin-crossover complex related to differences in intermolecular weak CH center dot center dot center dot X hydrogen bonds (X=S vs. S and N), *Chem. Commun.*, 2016, 52, 815–818; (g) V. A. Money, J. Elhaik, I. R. Evans, M. A. Halcrow and J. A. K. Howard, A study of the thermal and light induced spin transition in $[FeL_2](BF_4)_2$ and $[FeL_2](ClO_4)_2$ [L=2,6-di (3-methylpyrazol-1-yl)pyrazine], *Dalton Trans.*, 2004, 65–69; (h) G. S. Matouzenko, A. Bousseksou, S. A. Borshch, M. Perrin, S. Zein, L. Salmon, G. Molnar and S. Lecocq, Cooperative spin crossover and order-disorder phenomena in a mononuclear compound $[Fe(DAPP)(abpt)](ClO_4)_2$ [DAPP=bis(3-aminopropyl)(2-pyridylmethyl)amine, abpt=4-amino-3,5-bis( pyridin-2-yl)-1,2,4-triazole], *Inorg. Chem.*, 2004, 43, 227–236; (*i*) G. A. Craig, J. Sánchez Costa, O. Roubeau, S. J. Teat and G. Aromí, Coupled Crystallographic Order-Disorder and Spin State in a Bistable Molecule: Multiple Transition Dynamics, *Chem. – Eur. J.*, 2011, 17, 3120–3127; (*j*) M. Seredyuk, M. C. Muñoz, M. Castro, T. Romero-Morcillo, A. B. Gaspar and J. A. Real, Unprecedented multi-stable spin crossover molecular material with two thermal memory channels, *Chem. – Eur. J.*, 2013, 19, 6591–6596; (*k*) F. J. Valverde-Muñoz, M. Seredyuk, M. Meneses-Sánchez, M. C. Muñoz, C. Bartual-Murgui and J. A. Real, Discrimination between two memory channels by molecular alloying in a doubly bistable spin crossover material, *Chem. Sci.*, 2019, 10, 3807–3816.

16 (*a*) N. Ortega-Villar, M. Muñoz and J. Real, Symmetry Breaking in Iron(II) Spin-Crossover Molecular Crystals, *Magnetochemistry*, 2016, 2, 16; (*b*) M. Shatruk, H. Phan, B. A. Chrisostomo and A. Suleimenova, Symmetry-breaking structural phase transitions in spin crossover complexes, *Coord. Chem. Rev.*, 2015, 289–290, 62–73.

17 (*a*) E. Tailleur, M. Marchivie, N. Daro, G. Chastanet and P. Guionneau, Thermal spin-crossover with a large hysteresis spanning room temperature in a mononuclear complex, *Chem. Commun.*, 2017, 53, 4763–4766; (b) J. F. Létard, P. Guionneau, E. Codjovi, O. Lavastre, G. Bravic, D. Chasseau and O. Kahn, Wide thermal hysteresis for the mononuclear spin-crossover compound cis-bis (thiocyanato)bis[N-(2′-pyridylmethylene)-4-(phenylethynyl) anilino]iron(II), *J. Am. Chem. Soc.*, 1997, 119, 10861–10862.

18 D. Rosario-Amorin, P. Dechambenoit, A. Bentaleb, M. Rouzières, C. Mathonière and R. Clérac, Multistability at Room Temperature in a Bent-Shaped Spin-Crossover Complex Decorated with Long Alkyl Chains, *J. Am. Chem. Soc.*, 2018, 140, 98–101.

19 (*a*) M. Seredyuk, A. B. Gaspar, J. Kusz, G. Bednarek and P. Gütlich, Variable-temperature X-ray crystal structure determinations of {Fe[tren(6-Mepy)$_3$]}$(ClO_4)_2$ and {Zn[tren (6-Mepy)$_3$]}$(ClO_4)_2$ compounds: correlation of the structural data with magnetic and Mössbauer spectroscopy data, *J. Appl. Crystallogr.*, 2007, 40, 1135–1145; (*b*) M. Seredyuk, A. B. Gaspar, V. Ksenofontov, Y. Galyametdinov, J. Kusz and P. Gütlich, Does the solid-liquid crystal phase transition provoke the spin-state change in spin-crossover metallomesogens?, *J. Am. Chem. Soc.*, 2008, 130, 1431–1439; (*c*) M. Seredyuk, A. B. Gaspar, J. Kusz and P. Gütlich, Mononuclear complexes of iron(II) based on symmetrical tripodand ligands: novel parent systems for the development of new spin crossover metallomesogens, *Z. Anorg. Allg. Chem.*, 2011, 637, 965–976; (*d*) M. Seredyuk, Iron(II) metallomesogens based on symmetrical tripod ligands, *Inorg. Chim. Acta*, 2012, 380, 65–71; (*e*) S. Bonhommeau, P. G. Lacroix, D. Talaga, A. Bousseksou, M. Seredyuk, I. O. Fritsky and V. Rodriguez, Magnetism and molecular nonlinear optical second-order response meet in a spin crossover complex, *J. Phys. Chem. C*, 2012, 116, 11251–11255; (*f*) T. Delgado, A. Tissot, L. Guénée, A. Hauser, F. J. Valverde-Muñoz, M. Seredyuk, J. A. Real, S. Pillet, E.-E. Bendeif and C. Besnard, Very long-lived photogenerated high-spin phase of a multistable spin-crossover molecular material, *J. Am. Chem. Soc.*, 2018, 140, 12870–12876.

20 D. M. P. Mingos and A. L. Rohl, Size and shape characteristics of inorganic molecules and ions and their relevance to molecular packing problems, *J. Chem. Soc., Dalton Trans.*, 1991, 3419–3425.

21 C. Enachescu, R. Tanasa, A. Stancu, E. Codjovi, J. Linares and F. Varret, FORC method applied to the thermal hysteresis of spin transition solids: first approach of static and kinetic properties, *Physica B*, 2004, 343, 15–19.

22 J. F. Létard, P. Guionneau, O. Nguyen, J. S. Costa, S. Marcen, G. Chastanet, M. Marchivie and L. Goux-Capes, A guideline to the design of molecular-based materials with long-lived photomagnetic lifetimes, *Chem. – Eur. J.*, 2005, 11, 4582–4589.

23 P. Guionneau, F. Le Gac, S. Lakhoufi, A. Kaiba, D. Chasseau, J. F. Létard, P. Negrier, D. Mondieig, J. A. K. Howard and J. M. Leger, X-ray diffraction investigation of a spin crossover hysteresis loop, *J. Phys.: Condens. Matter*, 2007, 19, 11.

24 P. R. Spackman, M. J. Turner, J. J. McKinnon, S. K. Wolff, D. J. Grimwood, D. Jayatilaka and M. A. Spackman, CrystalExplorer: a program for Hirshfeld surface analysis, visualization and quantitative analysis of molecular crystals, *J. Appl. Crystallogr.*, 2021, 54, 1006–1011.

25 A. Alousy, J. Burgess and D. L. Elvidge, Solvation of iron(II) complexes of hexadentate tris-diimine Schiff base tripod ligands in alcohol–water and DMSO–water mixtures, *Transition Met. Chem.*, 2005, 30, 156–162.

26 K. Mierzejewska, M. Bochtler and H. Czapinska, On the role of steric clashes in methylation control of restriction endonuclease activity, *Nucleic Acids Res.*, 2016, 44, 485–495.

27 A. Bondi, van der Waals Volumes and Radii, *J. Phys. Chem.*, 1964, 68, 441–451.

28 M. A. Halcrow, Spin-crossover Compounds with Wide Thermal Hysteresis, *Chem. Lett.*, 2014, 43, 1178–1188.

29 (*a*) C. Cantin, J. Kliava, A. Marbeuf and D. Mikaïlitchenko, Cooperativity in a spin transition ferrous polymer: Interacting domain model, thermodynamic, optical and EPR study, *Eur. Phys. J. B*, 1999, 12, 525–540; (*b*) R. Boca, M. Bora, L. Dlhan, K. Falk, H. Fuess, W. Haase, R. Jarosciak, B. Papankova, F. Renz, M. Vrbova and R. Werner, Strong cooperativeness in the mononuclear iron(II) derivative exhibiting an abrupt spin transition above 400 K, *Inorg. Chem.*, 2001, 40, 3025–3033; (c) D. Chernyshov, N. Klinduhov, K. W. Törnroos, M. Hostettler, B. Vangdal and H. B. Bürgi, Coupling between spin conversion and solvent disorder in spin crossover solids, *Phys. Rev. B: Condens. Matter Mater. Phys.*, 2007, 76, 014406; (*d*) M. Mikolasek, W. Nicolazzi, F. Terki, G. Molnár and A. Bousseksou, Investigation of surface energies in spin crossover nanomaterials: the role of surface relaxations, *Phys. Chem. Chem. Phys.*, 2017, 19, 12276–12281; (*e*) M. Ndiaye, N. E. I. Belmouri, J. Linares and K. Boukheddaden, Elastic Origin of the Unsymmetrical Thermal Hysteresis in Spin Crossover Materials: Evidence of Symmetry Breaking, *Symmetry*, 2021, 13, 828.

30 G. Azzolina, R. Bertoni and E. Collet, General Landau theory of non-symmetry-breaking and symmetry-breaking spin transition materials, *J. Appl. Phys.*, 2021, 129, 085106.

31 M. G. Cowan, J. Olguín, S. Narayanaswamy, J. L. Tallon and S. Brooker, Reversible Switching of a Cobalt Complex by Thermal, Pressure, and Electrochemical Stimuli: Abrupt, Complete, Hysteretic Spin Crossover, *J. Am. Chem. Soc.*, 2011, 134, 2892–2894.

32 M. H. Lemée-Cailleau, C. Ecolivet, B. Ouladdiaf, F. Moussa, J. Jeftic and J. F. Létard, Intermediate ferroelastic phase of the photo-sensible spin-crossover system [Fe( ptz)$_6$]$(BF_4)_2$, *J. Magn. Magn. Mater.*, 2007, 310, 1792–1793.

33 E. Collet and G. Azzolina, Coupling and decoupling of spin crossover and ferroelastic distortion: Unsymmetric hysteresis loop, phase diagram, and sequence of phases, *Phys. Rev. Mater.*, 2021, 5, 044401.

34 C. P. Slichter and H. G. Drickamer, Pressure induced electronic changes in compounds of iron, *J. Chem. Phys.*, 1972, 56, 2142–2160.
35 J. F. Létard, Photomagnetism of iron(II) spin crossover complexes - the T(LIESST) approach, *J. Mater. Chem.*, 2006, 16, 2550–2559.
36 R. G. Miller, S. Narayanaswamy, S. M. Clark, P. Dera, G. B. Jameson, J. L. Tallon and S. Brooker, Pressure induced separation of phase-transition-triggered-abrupt vs. gradual components of spin crossover, *Dalton Trans.*, 2015, 44, 20843–20849.
37 (*a*) M. Seredyuk, A. B. Gaspar, V. Ksenofontov, S. Reiman, Y. Galyametdinov, W. Haase, E. Rentschler and P. Gütlich, Multifunctional materials exhibiting spin crossover and liquid-crystalline properties - Interplay between spin crossover and liquid-crystal properties in iron(II) coordination complexes, *Hyperfine Interact.*, 2005, 166, 385–390; (b) M. Seredyuk, K. Znovjyak, M. C. Muñoz, Y. Galyametdinov, I. O. Fritsky and J. A. Real, Imparting hysteretic behavior to spin transition in neutral mononuclear complexes, *RSC Adv.*, 2016, 6, 39627–39635; (c) F.-J. Valverde-Muñoz, M. Seredyuk, M. C. Muñoz, G. Molnár, Y. S. Bibik and J. A. Real, Thermochromic Meltable Materials with Reverse Spin Transition Controlled by Chemical Design, *Angew. Chem.*, 2020, 59, 18632–18638.